

Multichannel quantum defect calculation of the phase lag in the coherent control of HI

Hélène Lefebvre-Brion^{a)}

Laboratoire de Photophysique Moléculaire, Bâtiment 213, Université Paris-Sud,
91405 Orsay Cedex, France

Tamar Seideman

Steacie Institute for Molecular Sciences, National Research Council of Canada, Ottawa K1A 0R6, Canada

Robert J. Gordon

Department of Chemistry (m/c 111), University of Illinois at Chicago, Chicago, Illinois 60607-7061

(Received 22 December 2000; accepted 14 March 2001)

Multichannel quantum defect theory (MQDT) is applied within a unified framework to compute the ionization and dissociation channel phases of HI. Our numerical results illustrate the mathematical origin of a channel phase within the MQDT formalism, and are consistent with the existing theory of this phenomenon, based on the collision formalism and with experimental measurements. The present study explains why previous MQDT calculations predicted that the channel phase vanishes identically. © 2001 American Institute of Physics. [DOI: 10.1063/1.1370081]

I. INTRODUCTION

The channel phase, an observable in frequency domain coherent control experiments, has been the subject of intense interest during the past five years.^{1–11} The channel phase is the relative phase of two transition dipole elements leading from a given bound state into a continuum via two pathways,

$$\delta_{ab}^S = \arg \int d\hat{\mathbf{k}} \langle g | D_a | EnS\hat{\mathbf{k}}^- \rangle \langle EnS\hat{\mathbf{k}}^- | D_b | g \rangle, \quad (1)$$

where $|g\rangle$ is the initially prepared bound state, $|EnS\hat{\mathbf{k}}^- \rangle$ is an incoming-wave continuum eigenstate of energy E , correlating asymptotically with fragments in channel S , internal state n , and scattering vector $\hat{\mathbf{k}}$, and D_k ($k=a,b$) are two distinct dipole operators, corresponding to two different excitation modes.¹² In coherent control experiments¹³ the channel phase appears as a phase shift of the modulated yield curve,

$$p^S = p_a^S + p_b^S + 2|p_{ab}^S| \cos(\phi + \delta_{ab}^S), \quad (2)$$

where p_a^S and p_b^S are the probabilities of forming products in channel S via the noninteracting pathways, and ϕ is the relative phase of the laser fields. Although the absolute phase of the beat pattern is not an observable, it is possible to measure the phase lag, $\Delta \delta_{ab}(S, S') = \delta_{ab}^S - \delta_{ab}^{S'}$, between the modulation curves of two different product channels or processes, S and S' .

The first observation of a phase lag in 1- vs 3-photon control experiments¹ raised significant controversy in the theoretical literature.^{2–4} In this experiment, a molecular beam of HI molecules was simultaneously excited above the first ionization threshold with three UV photons of frequency ω_1 and one photon of frequency $\omega_3 = 3\omega_1$. The excited molecules decay both by ionization and dissociation. The iodine dissociation fragment was detected by ionization with an-

other ω_1 photon. The signals produced by HI^+ and I^+ , resulting, respectively, from the photoionization and photodissociation channels, were modulated by variation of the relative phase of the two laser beams.

Early analyses of the phase lag between these two signals argued that this quantity should vanish identically,^{2,3} or that it should vanish unless complex intermediates contribute to the multiphoton process.⁴ The experimental results, however, ruled out the latter mechanism. More recent theoretical work^{6,8} developed a general expression for the channel phase and established the relation of its energy dependence and the properties of the underlying continuum. By exploring several limits of the general expression, it was possible to rationalize the experimentally observed energy dependence of the channel phase as well as to make several predictions, a number of which have since been verified experimentally. It was shown, furthermore, that the channel phase could be applied to derive information about molecular continua, which is not available from more conventional observables.⁶ A numerical study of the channel phase in atomic ionization channels¹⁴ was found consistent with the theory.^{6,8}

Although the physical origin, structure, and information content of the channel phase of a general process are currently understood, numerical work has so far been limited to simple models⁶ and to atomic ionization channels.¹⁴ A numerical study of the competing ionization and dissociation reactions of HI, the system for which all experiments have been performed,^{1,5,7,9–11} has not been carried out as yet. The reason is clear. The spectroscopy of HI in the energy regime probed experimentally is complicated, involving spin-orbit autoionization, which has been treated by only a few authors.^{15,16} The dissociation dynamics has not been explored at all to our knowledge. The states responsible for predissociation of the resonance state have not been identi-

^{a)}Electronic mail: helene.lefebvre-brion@ppm.u-psud.fr

fied, and their structures are unknown. Also unknown is the magnitude and nature of electrostatic coupling within the scattering manifold. Below we suggest a possible assignment (that remains to be verified) of this predissociating state, based on recent experiments of Looock *et al.*¹⁷

One of the goals of the present work is to describe a method by which the two-step unified multichannel quantum defect theory (MQDT) of Refs. 18–24 can be adapted to compute the channel phases of competing ionization and dissociation channels. A second goal is to apply the method to model numerically the ionization and dissociation channel phases of HI. Our third goal is to clarify the reason for which previous MQDT calculations² predicted that the channel phase should vanish identically.

Our present study is preliminary in several ways. We consider a simplified model, consisting of an isolated resonance coupled to two continua, an ionization and a dissociation continuum, each of which is otherwise uncoupled. Rotations are omitted, and attention is confined to the regime of the $5d\delta$ Rydberg state of HI. These restrictions will be systematically relaxed in future work.

In the next section we outline the theory, and in Sec. III we present the numerical model and discuss the results. The final section concludes with an outlook to future research.

II. THEORY

With rotations neglected, the channel phase reduces, after integration over the scattering angles, to the relative phase of two distinct transition dipole operators between bound and unbound vibronic wave functions⁶ where, in the problem at hand, the unbound manifold decays into both an ionization and a dissociation continuum. These vibronic transition dipole elements are computed within the two-step unified MQDT framework.¹⁹

Following the standard quantum defect procedure, one partitions configuration space into a “reaction zone,” an inner region, and an external zone. Corresponding to this partitioning of space is a separation of the interaction into a short-range and a long-range part. One can write the total Hamiltonian H as

$$H = H_0 + H_2, \quad (3)$$

where

$$H_0 = T + H_{\text{LR}} + H_1, \quad (4)$$

and H_{LR} is the long-range potential. The reaction zone is defined by the range of electron-core interactions other than long-range (here Coulombic) forces. In the first step of the treatment, only H_0 is taken into account. The short-range interactions confined to a single electronic channel are contained in H_1 . The reaction matrix associated with H_1 is denoted by K_1 , and the induced phase shift is $\pi\mu$. In the second step of the treatment, the residual interactions between different channels are introduced through H_2 , which contains the part of the spin-orbit and electrostatic interactions not included in H_0 . The reaction matrix associated with the interchannel interactions is denoted by K_2 . The complete reaction matrix is the sum of K_1 and K_2 , and the scattering matrix takes a product form.

In the external region the ionization channel wave functions are expressed as superpositions of long-range (here Coulombic) functions,

$$\Psi_{iv}(r, R, \epsilon_i) = \chi_{iv} \Phi_i \{ f_l(\epsilon_i, r) \cos[\pi\mu_i(R)] - g_l(\epsilon_i, r) \sin[\pi\mu_i(R)] \}, \quad (5)$$

where R is the internuclear separation, r denotes the electronic coordinates, i is an electronic index, and v the vibrational quantum number. In Eq. (5) the χ_{iv} are bound vibrational functions, Φ_i are the core electronic functions, f_l and g_l are, respectively, the regular and irregular Coulomb functions, l being the electron angular momentum, μ_i are the quantum defects of the electronic continuum, and ϵ_i denotes the continuum electron energy with respect to the ion core.

The dissociative channels are given as

$$\Psi_d(r, R, \epsilon_d) = \Phi_d(r, R) F_d(\epsilon_d, R), \quad (6)$$

where Φ_d is a bound electronic wave function, and the F_d are energy normalized scattering solutions of the nuclear Schrödinger equation with total scattering energy ϵ_d above the dissociation limit. Equation (5) corresponds to bound motion in the nuclear modes, whereas Eq. (6) corresponds to bound motion of all electrons. The former includes both bound ($\epsilon_i < 0$) and free ($\epsilon_i > 0$) states in the electronic mode, distinguished by their asymptotic boundary conditions.

The short-range part of the electronic Hamiltonian, H_2 , couples the closed ($\epsilon_i < 0$) channels of Eq. (5) with both ionization and dissociation continua. Direct coupling of the ionization and dissociation continua was not included here but will be incorporated in a future study. The matrix elements of H_2 in the electronic basis,

$$V_{i,i'}^{(2)} = \langle \Phi_i \psi_i | H_2 | \Phi_{i'} \psi_{i'} \rangle \quad (7)$$

and

$$V_{i,d}^{(2)} = \langle \Phi_d | H_2 | \Phi_i \psi_i \rangle, \quad (8)$$

ψ_i being the radial function of the Rydberg electron in the reaction zone, are assumed independent of energy and internuclear separation. Because of the latter approximation, the matrix elements of the interaction in the vibronic basis, Eqs. (5) and (6), factorize into products of electronic and vibrational factors,

$$V_{iv,i'v'} = V_{i,i'}^{(2)} \langle \chi_{i,v} | \chi_{i',v'} \rangle (1 - \delta_{i,i'}) \quad (9)$$

and

$$V_{iv,d} = V_{i,d}^{(2)} \langle \chi_{iv} | F_d \rangle. \quad (10)$$

We proceed by defining a set of eigenchannels at the boundary of the reaction zone by diagonalizing the reaction matrix K_2 in the zero-order basis of Eqs. (5) and (6),

$$\Psi_\alpha = \sum_v U_{iv',\alpha} \chi_{iv} \Phi_i [f_l \cos(\pi\mu_i + \eta_\alpha) - g_l \sin(\pi\mu_i + \eta_\alpha)] + U_{d,\alpha} \Phi_d [F_d \cos \eta_\alpha - G_d \sin \eta_\alpha], \quad (11)$$

where U_α are eigenvectors of K_2 with components in both ionization and dissociation channels, $-\tan \eta_\alpha/\pi$ are the cor-

responding eigenvalues, and G_d is the second real solution of the nuclear Schrödinger equation, lagging in phase by $\pi/2$ with respect to F_d .

In the present work the reaction matrix K_2 is approximated within first-order perturbation theory and is thus obtained directly from the matrix elements of Eqs. (9) and (10). The energy eigenfunction outside the reaction zone, Ψ_ρ , is given as a linear superposition of the Ψ_α with coefficients A_α determined through application of the boundary conditions at infinity,

$$\Psi_\rho = \sum_\alpha A_\alpha \Psi_\alpha. \quad (12)$$

Finally, following the procedure of Refs. 18 and 19, the final open channel, F_{iv} , is given by a superposition of the energy eigenfunctions,

$$F_{iv} = \sum_\rho T_{iv,\rho} \Psi_\rho e^{i\tau_\rho}, \quad (13)$$

where

$$T_{iv,\rho} = \sum_\alpha A_\alpha^\rho \left[\sum_{v'} U_{iv',\alpha} [\cos(\pi\mu_i + \eta_\alpha) \langle \chi_{iv} | \chi_{iv'} \rangle] + U_{d,\alpha} \cos \eta_\alpha \langle \chi_{iv} | F_d \rangle \right] \cos \tau_\rho \quad (14)$$

$$+ \left[\sum_{v'} U_{iv',\alpha} [\sin(\pi\mu_i + \eta_\alpha) \langle \chi_{iv} | \chi_{iv'} \rangle] + U_{d,\alpha} \sin \eta_\alpha \langle \chi_{iv} | F_d \rangle \right] \sin \tau_\rho. \quad (15)$$

Using Eqs. (11) and (13), the matrix elements of the transition dipole operator, D_k in Eq. (1), between the initial vibronic state Φ_0 and the final open channel F_{iv} , are obtained as linear superpositions of the corresponding dipole elements between the initial vibronic state and the diabatic (single configuration) states of Eqs. (5) and (6),

$$D_{iv}^{(j)}(E) = \sum_\rho e^{i\tau_\rho} T_{iv,\rho} \sum_\alpha A_\alpha^\rho \left[\sum_{v'} \sum_{i'} U_{i'v',\alpha} D_{i'}^{(j)} \times \langle \chi_{v'} | \chi_0^0 \rangle + U_{d,\alpha} D_d^{(j)} \langle F_d | \chi_0^0 \rangle \right], \quad (16)$$

where

$$D_i^{(j)} = \langle \Phi_i | \psi_i | D^{(j)}(r) | \Phi_0 \rangle \quad (17)$$

and

$$D_d^{(j)} = \langle \Phi_d | D^{(j)}(r) | \Phi_0 \rangle, \quad (18)$$

$D^{(j)}$ being the j -photon transition dipole operator ($j=1$ or 3).

Before proceeding to compute the observable, we transform the single configuration transition dipole elements, $D_i^{(j)}$ in Eq. (16), from standing to traveling waves so as to impose implicitly the physical boundary conditions for the K_1 matrix.^{25,26} This last transformation was incorrectly omitted in previous MQDT formulations of similar problems.^{2,18} The use of standing wave dipole matrix elements has no conse-

quence when only total cross sections are computed. In the calculation of phase-sensitive observables, such as the channel phase, however, it is crucial to use the proper (traveling-wave) primitive dipole matrix elements, as shown below.²⁷

III. APPLICATION TO THE HI PROBLEM

We consider the simultaneous autoionization and predissociation of the $5d\delta 1/\sqrt{2}(^1\Pi_1 + ^3\Pi_1)$ Rydberg state of HI. This state converges on the $X^2\Pi_{1/2}$ state of the ion and autoionizes to the continuum of same symmetry of the $X^2\Pi_{3/2}$ ion state, namely $\epsilon d\delta 1/\sqrt{2}(^1\Pi_1 - ^3\Pi_1)$. Autoionization is due to spin-orbit interaction, and hence the coupling interaction in Eq. (7) assumes the form¹⁵

$$V^{(2)} = \tan \pi \left(\frac{\mu_1 - \mu_3}{2} \right), \quad (19)$$

where μ_1 and μ_3 are, respectively, the quantum defects of the singlet and triplet Rydberg states converging to the $^2\Pi_{1/2}$ continuum. Note that because of our choice of normalization of the wave function this interaction is dimensionless.

Simultaneous predissociation is due to electrostatic interaction with a repulsive neutral state of the same (Π) symmetry. Autoionization is known to be dominated by the ground vibrational levels of both the resonance and the ionic states, and in the present study we limit our attention to these levels.

The potential energy curve of the Rydberg resonance is taken to be parallel to that of the $X^2\Pi_{1/2}$ state, namely, a Morse potential with the parameters determined in Ref. 28 ($\omega_e = 2249.2 \text{ cm}^{-1}$, $\omega_e x_e = 50.8 \text{ cm}^{-1}$, and $r_e = 1.6228 \text{ cm}^{-1}$) up to $v=20$, but modified at higher energies to give the correct dissociation energy, $D_e = 25164 \text{ cm}^{-1}$. The ionization potential of $X^2\Pi_{3/2}$ used in these calculations is 83720 cm^{-1} , and the $X^2\Pi_{1/2}$ state lies 5356.6 cm^{-1} higher.²⁹⁻³¹ The quantum defect of the $d\delta$ resonance is taken equal to 0.162. With these parameters, the ground vibrational level of the $5d\delta$ resonance is located 541 cm^{-1} above the $v=0$ level of the $X^2\Pi_{3/2}$ state. The coupling matrix element between the two ionization channels [Eq. (19)] is taken to be 0.1.

The repulsive state responsible for predissociation of the Rydberg state is not known. Wigner-Witmer correlation rules suggest that this state has either $^1\Pi_1$ or $^3\Pi_1$ symmetry, and we assume that it dissociates into the $I^*(^2P_{3/2}) + \text{H}$ continuum at 80724.88 cm^{-1} , where I^* is $(^3P)6s$. A recent photofragment imaging study¹⁷ has presented evidence for a dissociative Rydberg state with a $^4\Sigma^-$ core and a $6p$ Rydberg electron at higher energy. This suggests that our dissociative state is a Rydberg state with the same $a^4\Sigma^-$ core (mixed by the spin-orbit operator with the $^4\Pi$ core) but with a $6s$ electron. Because one of the configurations of this repulsive state differs by two electrons from that of the $5d\delta$ resonance, an electrostatic interaction between these two states is possible. This coupling is estimated from the spectra of Hart and Hepburn³² using the following considerations: In Fig. 3 of Ref. 28 the peak corresponding to $n=5d(\pi+\delta)$ has a smaller intensity than the peak corresponding to $n=6d$. Theoretically, the autoionization peaks should have the same intensity (see, for example, Ref. 33). This intensity anomaly can be explained only if there is a local predisso-

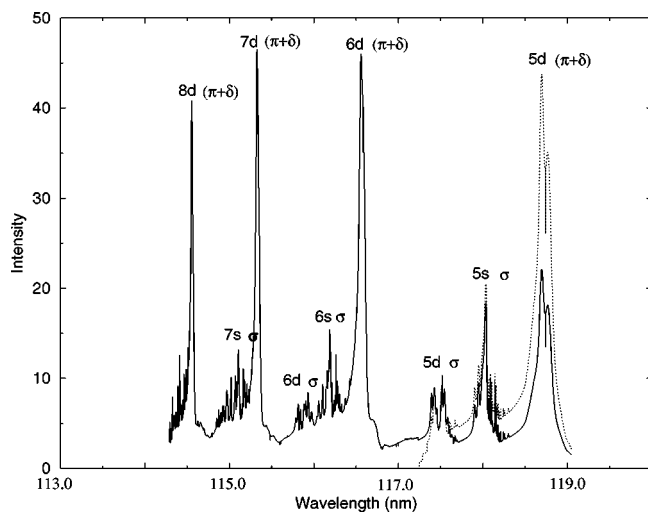


FIG. 1. Simulation of predissociation of the $5d\pi$ and $5d\delta$ resonances of HI at 300 K. The dotted curves were calculated assuming equal transition moments for all the n peaks. The solid curves were calculated with the transition moment for excitation of the $5d\pi$ state reduced by a factor of 1.4 and that for excitation of the $5d\delta$ state reduced by a factor of 2.1. See the text for further details.

ciation. A simulation of this predissociation is shown in Fig. 1. The dotted curves show the results of a MQDT calculation, accounting only for autoionization and including rotation in an intermediate coupling case between Hund's cases (a) and (e) (Ref. 34). The transition moments are taken such that the intensities for $5d\pi$ and $5d\delta$ would equal those of the higher ($n=6,7,8$) Rydberg states. The intensity of the $n=5$ peak is lowered with respect to that of the higher states if local predissociation that affects only the $5d\pi$ and $5d\delta$ states is taken into account in the simulation, as shown by the solid curves of Fig. 1. The experimental decrease of the intensity of the $5d\delta$ peak to about one-half that of the other peaks is reproduced with a dimensionless coupling of 0.124 for $\epsilon_d=4320\text{ cm}^{-1}$ [Eq. (10)], and this value is used in the calculation below.

The four electronic transition dipole matrix elements involved are not known. Because only their ratios are reflected in the observable, these elements serve as three independent adjustable parameters and are determined by a fit to the experimental phase lag data. The modulus of the one-photon transition moment element to the ionization channels is taken to be 1.58 a.u. The modulus of the three-photon element is systematically varied in the 0.1–1.0 a.u. range to optimize agreement with experiment. A value of 0.6 a.u. is determined through this procedure and employed in the calculation. The modulus of the one-photon transition moment element to the dissociative state is varied in the 0.1 to 0.2 a.u. range, and that of the three-photon transition moment element is varied between ± 0.05 and ± 0.005 a.u. The values of 0.1 and -0.03 a.u. for the one- and three-photon transition moments, respectively, are found to produce best agreement with experimental data. Our model potential energy curves are given in Fig. 2.

The cross sections for ionization and for dissociation are shown in Fig. 3 for one-photon excitation.

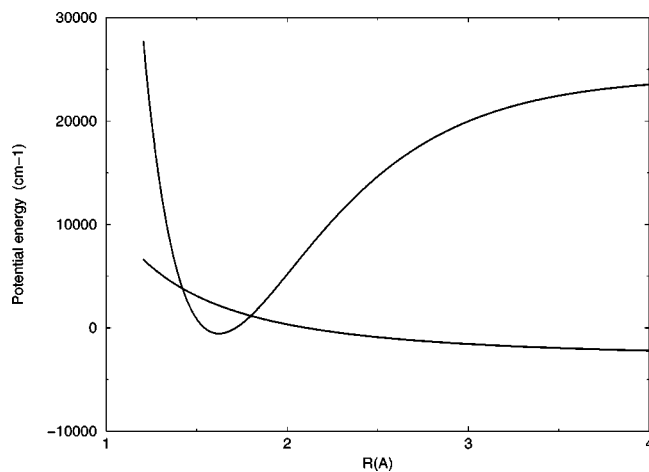


FIG. 2. Model potential energy curves for the $5d\delta$ state and for the state responsible for predissociation.

IV. RESULTS AND DISCUSSION

We first recall that previous MQDT calculations predicted that the channel phase for both ionization and dissociation vanishes identically, in contradiction with the theory of Refs. 6 and 7 and with observations. The source of this discrepancy is the use of standing wave primitive transition dipole elements in Ref. 2. This effect is readily seen by examining Eq. (16). In the case considered here, where only two channels are involved, one open and one closed, Eq. (16) simplifies to

$$D_{iv}^{(j)}(E) = e^{i\tau_p} T_{iv,\rho} 2^{-1/2} [A_1^\rho (D_1^{(j)} - D_2^{(j)}) + A_2^\rho (D_1^{(j)} + D_2^{(j)})], \quad (20)$$

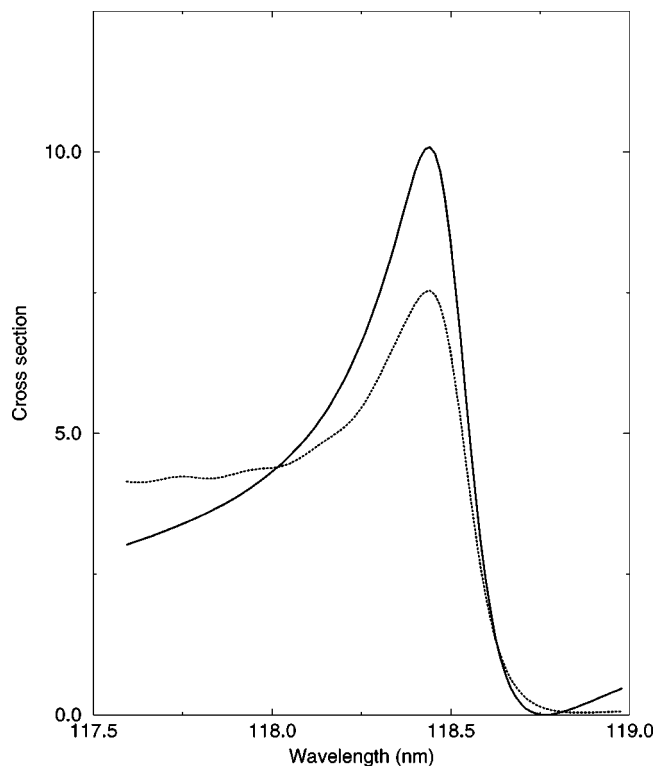


FIG. 3. Ionization (solid curve) and dissociation (dotted curve) one-photon cross sections in the regime of the $5d\delta$ resonance.

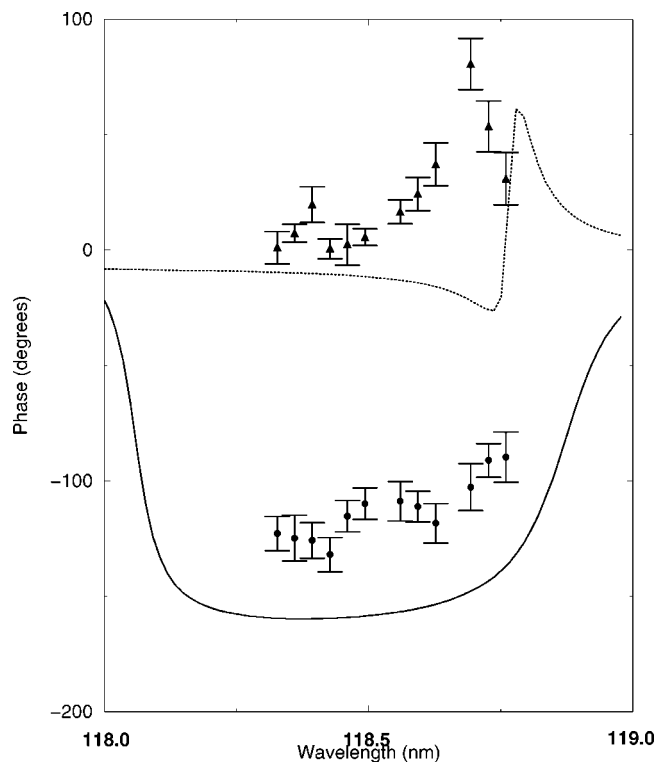


FIG. 4. The solid and dashed curves are, respectively, the calculated channel phases for dissociation and ionization via the $5d\delta$ resonance. The circles and triangles are the corresponding experimental values (see Ref. 10). Error bars indicate one standard deviation for typically ten measurements.

where $D_1^{(j)}$ and $D_2^{(j)}$ are, respectively, the primitive electronic transition moment elements to the zero-order discrete and continuum states. If the standing wave electronic elements are used, the phases of $D_{iv}^{(1)}(E)$ and $D_{iv}^{(3)}(E)$ both equal τ_ρ , and the channel phase accordingly vanishes.

When the proper traveling wave boundary conditions are imposed,²⁵ i.e., when ψ_i in Eq. (17) is replaced by²⁶

$$\psi_i^S = \sum_j \psi_j Q_{ji}, \quad (21)$$

where \mathbf{Q} is the complex matrix $(\mathbf{1} - iK_1)^{-1}$, we find that the ionization channel phase is nonzero, irrespective of whether the autoionization MQDT or the autoionization +predissociation MQDT is used. Considering first the ionization process alone within the former framework, we find an ionization channel phase that is constant with energy and depends on the phase of the primitive transition moments. If, however, the transition moment for the direct and resonance-mediated ionization pathways differ slightly, a Lorentzian curve is obtained in agreement with the prediction of Ref. 8 (for the case of an isolated resonance embedded in an otherwise uncoupled continuum considered here) and consistent with experiment.¹³ The choice of unequal transition moment is physically correct; it follows if the approximation of energy-independence of the transition moment is relaxed because ϵ_i differs for the $^2\Pi_{3/2}(\epsilon_i > 0)$ and the $^2\Pi_{1/2}(\epsilon_i < 0)$ cores (see Ref. 35 for the energy dependence of the photoionization cross section).

Considering next the predissociation problem alone, we have verified that the channel phase is nonzero and takes the shape predicted in Ref. 8 for the model considered here. It vanishes when the transition dipole element to the repulsive state is set to zero. Thus as the frequency is tuned to the vicinity of the center of an isolated resonance and the resonance-mediated process becomes dominant, the channel phase decreases to a minimum, consistent with previous theory and with observations.^{5,6}

Continuing to include both the ionization and the dissociation channels within a unified MQDT simulation, we find that the ionization channel phase is modified from the result of the MQDT simulation with only one open channel. This result is expected because, with the dissociation channel included, an additional source of interference is introduced, interference between two continua, that was identified in earlier work^{5,6} as a source of a channel phase. Here the coupling between the two continua is indirect, mediated through the resonance. The ionization phase is constant, except in the vicinity of the resonance where it has a dispersion-like shape.

Within the unified MQDT, the dissociation phase takes a Lorentzian shape. The indirect interaction with the ionization continuum has only a minor effect. Experimentally one observes a rather different shape, indicative of coupling in the dissociation manifold, which our present model does not account for.

We have used for the primitive complex transition moments to the two ionization channels a value of $1.5 + 0.496i$ for the one-photon transition and $0.593 + 0.09i$ for the three-photon transition, corresponding to the moduli of 1.58 and

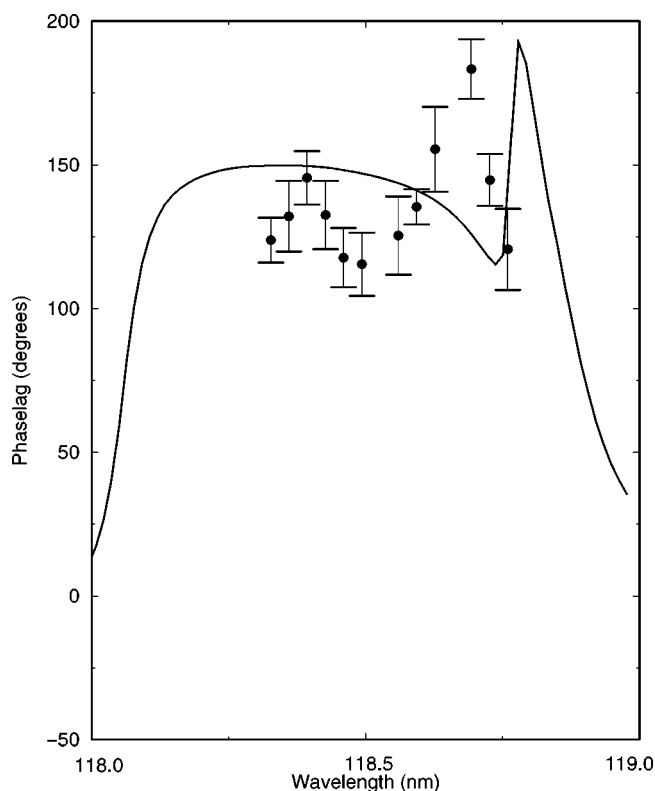


FIG. 5. The solid curve is the calculated phase lag (ionization–dissociation) in the region of the $5d\delta$ resonance; the circles and error bars are the corresponding experimental measurements.

0.6 a.u., respectively. The channel phases for both the ionization and dissociation of HI, obtained within the unified MQDT simulation, are plotted in Fig. 4 versus the one-photon wavelength. Also shown in Fig. 4 are the experimental ionization and dissociation channel phases in the same region. The experimental channel phase was obtained from measurement of the phase lag between the process of interest and a process known to produce no channel phase, as discussed in Ref. 9.

In Fig. 5 we show the calculated phase lag between the ionization and dissociation channels in the vicinity of the $5d\delta$ resonance and compare it with the measurement of Ref. 7. A maximum of 180° is obtained, which agrees with the experiment in magnitude but lies at slightly too low an energy. The second maximum in the experimental data at 118.4 nm is probably due to the $9d$ resonance with a $^2\Pi_{3/2} v=1$ (Ref. 36) core, which has not been introduced in the calculation. A more complete spectroscopic assignment of the phase lag spectrum will be forthcoming.³⁷

V. CONCLUSIONS

We present MQDT calculations of the ionization and dissociation channel phases of HI. Our results explain the reason for which previous MQDT calculations incorrectly predicted that the channel phase should vanish identically. In the case that a single decay channel is open (i.e., for an elastic continuum), when standing wave boundary conditions are improperly used, the channel phase is strictly zero. Incorporating the correct, traveling wave boundary conditions gives rise to a channel phase that agrees in structure with the current theory of the phase lag phenomenon and with observations. If the resonance has a symmetric profile (i.e., for $q \rightarrow \infty$), the phase lag is identically zero, again, in agreement with the existing theory and with experimental results.

In the present study we considered the case of spin-orbit autoionization, pertaining to the existing experimental data. It would be interesting to study both theoretically and experimentally resonances that can decay by autoionization mechanisms other than spin-orbit interaction. Problems where autoionization and predissociation take place on comparable time scales are of particular interest. (See Ref. 38 for a review of this subject.)

Our model has neglected effects of coupling between continuum channels, overlapping resonances, and rotations. Extending the present study to account for these effects is another goal of future work.

ACKNOWLEDGMENTS

The authors thank Dr. Annick Suzor-Weiner for her critical reading of the manuscript. All the calculations reported in this work were carried out at the French National Computer Center (CINES). R.J.G. gratefully acknowledges support by the National Science Foundation.

- ¹L. Zhu, V. D. Kleiman, X. Li, L. Lu, K. Trentelman, and R. J. Gordon, *Science* **270**, 77 (1995).
 - ²H. Lefebvre-Brion, *J. Chem. Phys.* **106**, 2544 (1997).
 - ³T. Nakajima, J. Zhang, and P. Lambropoulos, *J. Phys. B* **30**, 1077 (1997).
 - ⁴S. Lee, *J. Chem. Phys.* **107**, 2734 (1997); **108**, 3903 (1998).
 - ⁵L. Zhu, K. Suto, J. A. Fiss, R. Wada, T. Seideman, and R. J. Gordon, *Phys. Rev. Lett.* **79**, 4108 (1997).
 - ⁶T. Seideman, *J. Chem. Phys.* **108**, 1915 (1998).
 - ⁷J. A. Fiss, A. Khachatryan, L. Zhu, R. J. Gordon, and T. Seideman, *Discuss. Faraday Soc.* **113**, 61 (1999).
 - ⁸T. Seideman, *J. Chem. Phys.* **111**, 9168 (1999).
 - ⁹J. A. Fiss, L. Zhu, R. J. Gordon, and T. Seideman, *Phys. Rev. Lett.* **82**, 65 (1999).
 - ¹⁰J. A. Fiss, A. Khachatryan, K. Truhins, L. Zhu, R. Gordon, and T. Seideman, *Phys. Rev. Lett.* **85**, 2096 (2000).
 - ¹¹J. A. Fiss, L. Zhu, K. Suto, G. He, and R. J. Gordon, *Chem. Phys.* **233**, 335 (1998).
 - ¹²M. Shapiro, J. W. Hepburn, and P. Brumer, *Chem. Phys. Lett.* **149**, 451 (1988).
 - ¹³For reviews see: R. J. Gordon, L. Zhu, and T. Seideman, *Acc. Chem. Res.* **32**, 1007 (1999); *Comments At. Mol. Phys.* (in press); *J. Phys. Chem.* (submitted).
 - ¹⁴P. Lambropoulos and T. Nakajima, *Phys. Rev. Lett.* **82**, 2266 (1999).
 - ¹⁵H. Lefebvre-Brion, A. Giusti-Suzor, and G. Raseev, *J. Chem. Phys.* **83**, 1557 (1985).
 - ¹⁶A. Mank, M. Drescher, T. Huth-Fehre, N. Böwering, U. Heinzmann, and H. Lefebvre-Brion, *J. Chem. Phys.* **95**, 1676 (1991).
 - ¹⁷H. P. Loock, B. L. G. Bakker, and D. H. Parker, *Can. J. Phys.* (Herzberg special issue, to be published in 2001).
 - ¹⁸A. Giusti-Suzor and H. Lefebvre-Brion, *Chem. Phys. Lett.* **76**, 132 (1980). Note that, in this paper, Eq. (8) should be written
- $$D_v^j(E) = \sum_{\rho} e^{i\tau_{\rho} T} T_{jv,\rho} \sum_{\alpha} \sum_{v'} \sum_i U_{i v', \alpha} A_{\alpha}^{\rho} \int \chi_{v'}(R) D_i(R) \chi_0^0(R) dR.$$
- ¹⁹A. Giusti, *J. Phys. B* **13**, 3867 (1980).
 - ²⁰A. Giusti-Suzor and Ch. Jungen, *J. Chem. Phys.* **80**, 986 (1984).
 - ²¹H. Lefebvre-Brion and F. Keller, *J. Chem. Phys.* **90**, 7176 (1989).
 - ²²A. J. Yencha, D. Kaur, R. J. Donovan, A. Kvaran, A. Hopkirk, H. Lefebvre-Brion, and F. Keller, *J. Chem. Phys.* **99**, 4986 (1993).
 - ²³H. Lefebvre-Brion, M. Salzmann, H.-W. Klausing, M. Müller, N. Böwering, and U. Heinzmann, *J. Phys. B* **22**, 3851 (1989).
 - ²⁴A. J. Yencha, A. Hopkirk, J. R. Grover, B.-M. Cheung, H. Lefebvre-Brion, and F. Keller, *J. Chem. Phys.* **103**, 2882 (1995).
 - ²⁵R. G. Newton, *Scattering Theory of Waves and Particles* (McGraw-Hill, New York, 1966).
 - ²⁶G. Raseev, A. Giusti-Suzor, and H. Lefebvre-Brion, *J. Phys. B* **11**, 2735 (1978).
 - ²⁷Note that in a paper published in *Phys. Rev.* **184**, 250 (1969), U. Fano pointed out that he had made a similar error in a previous calculation of the photoelectron spin polarization.
 - ²⁸N. Böwering, H.-W. Klausing, M. Müller, M. Salzmann, and U. Heinzmann, *Chem. Phys. Lett.* **189**, 467 (1992).
 - ²⁹A more accurate value of the ionization potential of HI is $83\,750 \pm 1 \text{ cm}^{-1}$, which is obtained by subtracting the spin-orbit splitting of Ref. 30 from the energy of the $\text{HI}^+ X^2\Pi_{3/2}$ state reported in Ref. 31.
 - ³⁰A. Chanda, W. C. Ho, F. W. Dalby, and I. Ozier, *J. Chem. Phys.* **102**, 8725 (1995).
 - ³¹S. T. Pratt, *J. Chem. Phys.* **101**, 8302 (1994).
 - ³²D. J. Hart and J. W. Hepburn, *Chem. Phys.* **129**, 51 (1989).
 - ³³H. Lefebvre-Brion and R. W. Field, *Perturbations in the Spectra of Diatomic Molecules* (Academic, Orlando, FL, 1986).
 - ³⁴H. Lefebvre-Brion, in *High Resolution Laser Photoionization and Photoelectron Studies*, edited by I. Powis, T. Baer, and C. Y. Ng (Wiley, New York, 1995), p. 171.
 - ³⁵H. Lefebvre-Brion, G. Raseev, and H. Le Rouzo, *Chem. Phys. Lett.* **123**, 341 (1988).
 - ³⁶H. Lefebvre-Brion (unpublished calculations).
 - ³⁷A. Khachatryan, R. Bilotto, R. J. Gordon, T. Seideman, and H. Lefebvre-Brion (unpublished results).
 - ³⁸H. Lefebvre-Brion and A. Suzor-Weiner, *Comments At. Mol. Phys.* **29**, 305 (1994).